# DESIGN AND FABRICATION OF HIGH TEMPERATURE RESISTIVITY MEASUREMENT SETUP

Thesis Submitted for the Award of the Degree of

***Master of Science***

By

***KALYANI BHOI***

Under the academic autonomy

***National Institute of Technology, Rourkela***

Under the Guidance of

***Dr. Prakash Nath Vishwakarma***
***&***
***Dr. Dillip Kumar Pradhan***


***Department of Physics***

***National Institute of Technology***

***Rourkela-769008***

# DECLARATION

I hereby declare that the project work entitled " **Design and fabrication of high temperature resistivity measurement setup**" submitted to National Institute of Technology, Rourkela is a record of original work by me under the guidance of Dr. Dillip Kumar Pradhan and Dr. Prakash Nath Vishwakarma, Assistant Professors, Department of Physics, N.I.T Rourkela. This project work has not performed the basis for the award of any Degree or diploma/ associate ship/fellowship and similar project if any.

**KALYANI BHOI**
Roll no. 409ph2084
M Sc. Physics
N.I.T Rourkela

**Department of Physics**

**National Institute of Technology**

**Rourkela – 769008 (Orissa)**

# CERTIFICATE

This is to certify that the thesis entitled "**Design & Fabrication of High Temperature Resistivity Measurement Setup**" submitted by **Kalyani Bhoi** in partial fulfilment of the requirements for the award of degree of Master of Science in Physics at National Institute of Technology, Rourkela is an authentic work carried out by her under our supervision. To the best of my knowledge, the work done under this thesis has not been submitted by any other university/ Institute for the award of any degree or diploma.

Dr. Prakash Nath Vishwakarma

Dr. Dillip Kumar Pradhan

# ACKNOWLEDGEMENT

First and foremost, to my friend, pew mate and my collaborator, Sushree Rosyla Barpanda for working so hard for this project and standing there for me in all my ups and downs.

I am heartily thankful to my supervisor, Dr. Dillip Kumar Pradhan and Dr. Prakash Nath Vishwakarma , whose encouragement, supervision and support from the preliminary to the concluding level enabled me to develop an understanding of the subject.

I cannot fully express my gratitude to the exceptional team at Department of Physics, NIT Rourkela, including all my friends. I am extremely thankful to Barun Kumar Barick, Jashashree Ray and Achyuta kumar Biswal, Ph.D Scholar of Department of physics, NIT Rourkela, for their help in result analysis and computer interfacing with the set up.

For the generous assistance in the research of this project, I would like to acknowledge the Central Workshop for extending their facilities for preparing my setup, Department of Chemistry for providing the required materials for my sample preparation and Department of Metallurgical and Material Science for the help in taking XRD.

I humbly prostrate myself before the Almighty for his grace and abundant blessings, which enabled me to complete this work successfully.

Last but not least I wish to avail myself of this opportunity, express a sense of gratitude and love to my beloved parents and my family for their manual support, strength, help and for everything.

**KALYANI BHOI**

**DEDICATED TO MY PARENTS**

# TABLE OF CONTENTS

LIST OF TABLES……7

LIST OF FIGURES……..7

ABSTRACT……..9

1. INTRODUCTION……..10

1.1 ORIGIN OF RESISTANCE…….10

1.2 RESISTIVITY……..12

1.3 RESISTIVITY MEASUREMENT METHOD……15

1.4 RESISTANCE TEMPERATURE DETECTOR(RTDs)…….17

1.5 THERMOCOUPLE……..20

2. INSTRUMENT DESIGNING……27

2.1 FURNACE DESIGNING…….27

2.2 FOUR PROBE WITH SAMPLE HOLDER…….....35

3. SAMPLE PREPARATION……38

3.1 CHOICE OF SAMPLE…….38

3.2 APLLICATION OF CFO…….38

3.3 SAMPLE SYSTHESIS…….40

4. RESULTS AND DISCUSSION…….43

4.1 SAMPLE CHARACTERISATION……..43

4.2 WILLIAMSON HALL METHOD……...44

4.3 RESISTIVITY MEASYREMENT……...45

4.4 CALCULATION OF ACTIVATION ENERGY……..46

5. CONCLUSION AND FUTURE SCOPE OF RESEARCH……..47

APPENDIX……...49

REFERENCES……..52

# LIST OF TABLES

1.1 Resistivity of various materials……14
1.2 Resistivity of common RTDs……18
1.3 Types of thermocouple and their properties……26

# LIST OF FIGURES

1.1 Resistivity of a material.....13
1.2 Movement of electron in a) cold body b) hot body.....13
1.3 Resistivity vs. Temperature graphs for a) conductor b) semiconductor
c) superconductor.....14
1.4 Schematic diagram for two probe.....15
1.5 Schematic diagram for four probe.....16
1.6 Van der Pauw measurement at different configuration.....16
1.7 Platinum resistance thermometer a) Pt-100 probe b) schematic representation.....19
1.8 Plot of resistivity vs. temperature of Pt-100……..20
1.9 Al-Cu Thermocouple for Seebeck effect…….....21
1.10 Thermo-emf vs. Temperature of a thermocouple.....23
1.11 Thermoelectric junction for Peltier effect.....23
1.12 Free electron model of thermocouple behaviour ……25
2.1 Interior of the designed furnace.....28
2.2 Block diagram of the furnace.....29
2.3 Graphical representation of proportional control system.....30
2.4 Graphical representation of integral control system.....31
2.5 Graphical representation of derivative control system.....32
2.6 Calibration of furnace at different power and set temperature.....33
2.7 Furnace with temperature controller.....34
2.8 Four probe assembly.....36
2.9 Block diagram of the designed resistivity set-up.....37
3.1 Schematic illustration of removal cancer cell by application of external magnetic field on magnetic nanoparticle capped with $SiO_2$ .....38

3.2 Microwave sensor product…….....40
3.3 Flowchart for CFO preparation….....42
4.1 X-ray diffraction pattern of CFO.....43
4.2 Williamson Hall plot for CFO.....44
4.3 Resistivity vs. Temperature graph of CFO.....45
4.4 Arrhenius plot for resistivity data of CFO.....46

# ABSTRACT

A high temperature resistivity measurement set-up has been designed consisting of a furnace and a four probe to measure the resistivity of prepared sample. The handmade furnace can withstand temperature up to $600^0$C. The system also consists of an automatic temperature controller which uses the principle of an 'on-off' furnace controller. K-type thermocouple is used to measure the furnace temperature and a Pt-100 sensor is used for sample temperature measurement. This Pt-100 sensor is connected with digital multimeter which gives its corresponding resistances for temperature conversion. The setup is connected with Keithley nanovolmeter and Keithley current source which are interfaced with the computer using Lab-view software. This arrangement reduces the manual effort. In this experimental set up, both bulk and thin film samples can be investigated, making it versatile. We have prepared a ceramics oxide by soft chemical method and the formation of the compound has been checked using X-ray diffraction analysis. The crystal structure is found to be cubic with lattice parameter a = $8.391A^0$. The temperature dependent resistivity of the ceramic oxide sample is presented as a test material to demonstrate the possibility and accuracy of the experimental set-up. The temperature dependent electrical resistivity follows Arrhenius behaviour.

# CHAPTER 1

## INTRODUCTION

The modern concept of electrical resistance was first discovered by G. S. Ohm, in 1926, who formulated the famous equation relating voltage and current while working on direct-current circuit.

V=IR (Ohms law)

The resistance is a function of temperature and stress for a given material. This property of resistance is employed in resistance-temperature conversion.

## 1.1 ORIGIN OF RESISTANCE :

The electrical resistance of an object is a measure of its opposition to the passage of an electric current. Electrical resistance of a circuit component or device is defined as the ratio of the voltage applied to the electric current which flows through it.

$$R = \frac{V}{I}$$


The SI unit of electrical resistance is the ohm (Ω). The reciprocal quantity of resistance is electrical conductance which is measured in Siemens.

### 1.1.1 Causes of resistance:

**In metals:**

When voltage (electrical potential difference) is applied across a metal, the electrons drift from one end of the conductor to the other. Near room temperatures, the thermal motion of ions is the primary source of scattering of electrons, and is thus the prime cause of metal resistance. Imperfections of lattice also contribute into resistance, although their contribution in pure metals

is negligible. Longer conductors have more scattering events in each electron's path, so the higher is the resistance [1].

**In semiconductor and insulator:**

In semiconductors, the Fermi level lies within the band gap, approximately half-way between the conduction band minimum and valence band maximum for intrinsic (undoped) semiconductors. So at zero Kelvin, there are no free conduction electrons and the resistance is infinite. However, the resistance decreases as the charge carrier density in the conduction band increases. In extrinsic (doped) semiconductors, dopant atoms increase the majority charge carrier concentration by donating electrons to the conduction band or accepting holes in the valence band. For both types of donor or acceptor atoms, increasing the dopant density leads to a reduction in the resistance. That is the reason behind the metallic behaviour of highly doped semiconductors. At very high temperatures, the contribution of thermally generated carriers will dominate over the contribution from dopant atoms and the resistance will decrease exponentially with temperature [1].

**In superconductors:**

At a certain temperature (critical temperature), the electrical resistance of some metals and ceramic materials, becomes zero. These materials are called superconductor. In a superconductor below its critical temperature, resistance is zero because the scattering mechanisms are unable to impede the motion of the current carriers. As a negatively-charged electron moves through the space between two rows of positively-charged atoms, it interacts with another electron by exchanging acoustic quanta called phonon. This distortion attracts a second electron to move in behind it. The two electrons form a weak attraction, travel together in a pair and encounter less resistance overall. The current is carried then by electrons moving in pairs called Cooper pairs. So they can carry large amounts of electrical current for long periods of time without losing energy as ohmic heat [2].

### 1.1.2 Temperature dependence of resistance:

Near room temperature, the electrical resistance of a typical metal increases linearly with increase in temperature, while the electrical resistance of a typical semiconductor decreases with rising temperature. The amount of the change in resistance can be calculated using the temperature coefficient of resistivity of the material using the following relation.

$$R = R_o + \left[\alpha\left(T - T_o\right) + 1\right]$$

Where,

$T$ is its temperature,

$T_0$ is a reference temperature (usually room temperature),

$R_0$ is the resistance at $T_0$, and

$\alpha$ is the temperature coefficient of resistance.

The constant $\alpha$ depends only on the material being considered.

Intrinsic semiconductors become better conductors as the temperature increases. The electrons jumps to the conduction energy band by thermal energy, where they flow freely and leave behind holes in the valence band which also flow freely. The electric resistance of a typical intrinsic (non doped) semiconductor decreases exponentially with rise in temperature:

$$R = R_o e^{-\alpha T}$$

Extrinsic (doped) semiconductors have a complicated temperature profile. As temperature increases starting from absolute zero, they first decrease steeply in resistance as the carriers leave the donors or acceptors. At higher temperatures it will behave like intrinsic semiconductors as the carriers from the donors/acceptors become insignificant compared to the thermally generated carriers [1].

## 1.2 RESISTIVITY

The quantitative measure of a material's opposition to the flow of current is called resistivity. It depends only on the composition of the material and not on the shape and size.

$$R = \frac{\rho L}{A}$$

Where,
R is the resistance (ohms),

ρ is resistivity (ohm-meters),

L is the length (meters), and

A is the cross-sectional area (square-meters).

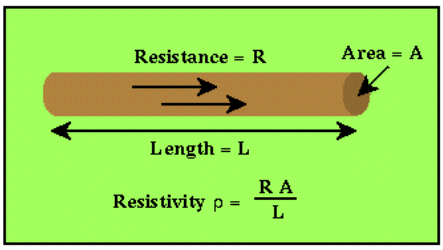


**Fig 1.1: Resistivity of a material [3]**

The resistivity of the material changes with temperature. For many materials, the change is a simple linear function of temperature,

$$\rho(T) = \rho_0[1 - \alpha(T - T_0)]$$

Where,

ρ(T) is the resistivity at temperature T,

$\rho_0$ is the resistivity at temperature $T_0$,and

α is the temperature coefficient of resistivity.

Although it is temperature dependent, it can be used to calculate the resistance of a wire of given geometry at a given temperature. [4]

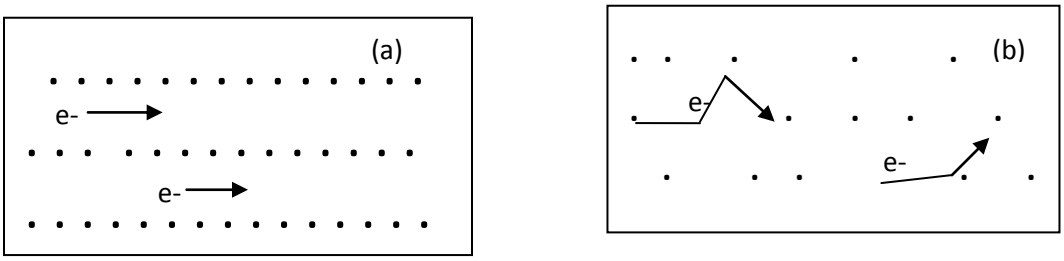


**Fig 1.2: movement of electron in (a) cold body (b) hot body.**

| Material | Resistivity, ρ(ohm-meter) |
|---|---|
| Metals | $10^{-8}$ |
| Semiconductors | Variable |
| Electrolytes | Variable |
| Insulators | $10^{16}$ |
| Superconductors | 0(exactly) |

**Table 1.1:Resistivity of various materials.**

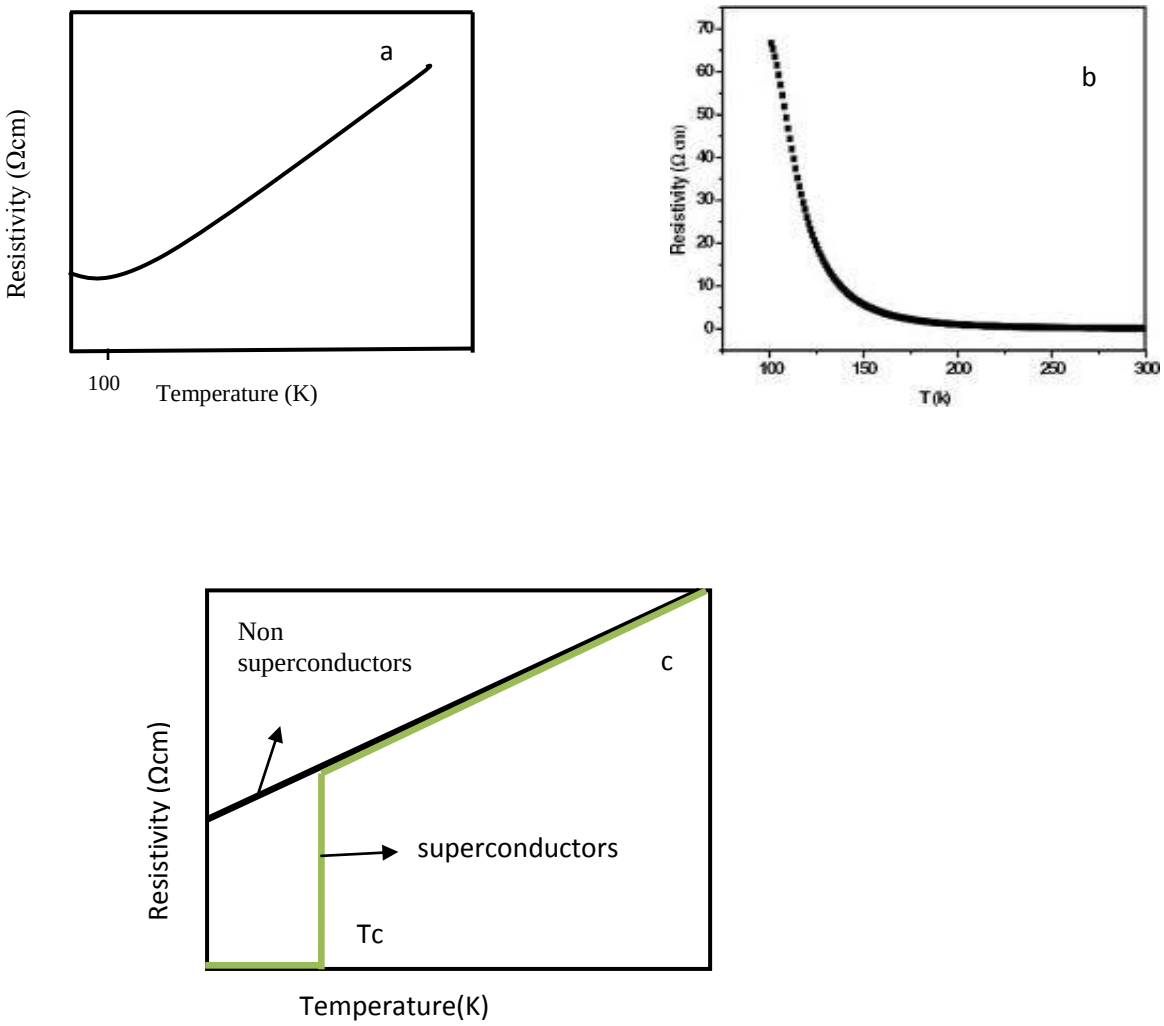


**Fig 1.3: Resistivity vs. temperature graphs for a) conductor, b) semiconductor and c) superconductor.**

The resistivity of the various materials is listed in table 1.1. The temperature dependence of resistivity of the various materials is shown in Figure 1.3.

## 1.3 RESISTIVITY MEASUREMENT METHODS

The resistivity is determined by measuring resistance R and the dimensions of the sample (length l, width/ thickness d). The resistance R is usually determined by a voltage-current method. A current of known 'I' value is fed into the sample and the voltage 'V' is measured via point contact.

From these measurements the resistivity is calculated as,

$$\rho = R\frac{w \times d}{l}$$

There are various methods of resistivity measurements:

### 1.3.1 Two probe method:

The test specimen for the two probe method may be in the form of strip, rod or bar. The two probe method always gives a value with contributions from contact wires, contact resistance and hence not advisable in case of metals where the sample resistance is very low.

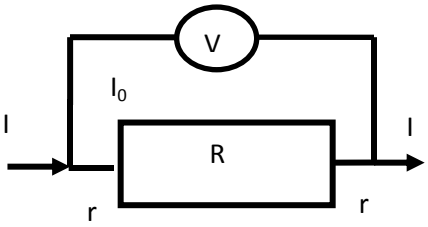


**Fig 1.4: schematic diagram of two probe.**

Since the internal resistance of voltmeter is very high ($10^6$ Ω), hence $I_0 << I$, so that $I - I_0 \sim I$. So the voltage measured by the voltmeter will be,

$$= (I - I_0)(r + R + r).$$

So, r+R+r gives an error to the measurement. However this method can be applied (if R>>2r) for highly resistive samples.

### 1.3.2 Four probe method:

Four probe method minimizes the other contributions (lead resistance, contact resistance, etc.) to the resistance measurement which results in an accurate measurement of sample resistance. This includes four equally spaced probes in contact with a material of unknown resistance. The outer two probes are used for sourcing the current and the two inner probes are used for measuring the resulting voltage drop across the surface of the sample.

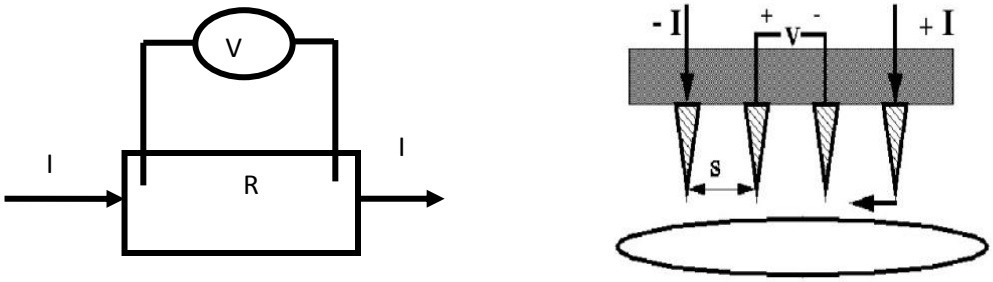


**Fig 1.5: schematic diagram of four probe.**

Here according to the diagram, the voltage measured by the voltmeter is

$$= (I-I_0)R$$

Hence, the voltage measured is more accurate without any error in four probe.

### 1.3.3 Van der Pauw method:

This technique is commonly used for measuring sheet resistance of a material. For samples of irregular shape and size, the two and four probe method is not applicable and so choice is Van der Pauw method. This method includes the measurement of two resistance, $R_A$ and $R_B$ as shown in the figure given below.

$R_A=V_{43}/I_{12}$

$R_B=V_{14}/I_{23}$

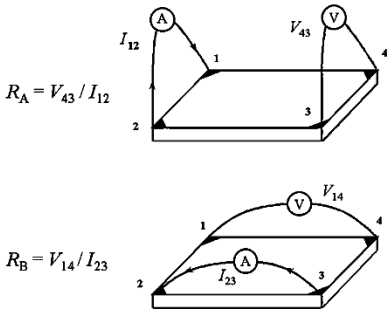


**Fig 1.6 : Van-der Pauw measurement in different configurations**

The sheet resistance is related to these calculated resistances by the van der pauw formula,

$$e^{\frac{-\pi R_A}{R_s}} + e^{\frac{-\pi R_B}{R_s}} = 1$$

where, $R_s$ is sheet resistance to be determined. If $R_A$ and $R_B$ are similar, then resistivity is given by,

$$\rho = \frac{\pi d}{\ln 2} \frac{(R_A + R_B)}{2}$$

where, d is the thickness of the sample. If $R_A$ and $R_B$ are not similar then resistivity modifies as,

$$\rho = \frac{\pi d}{\ln 2} \frac{(R_A + R_B)}{2} f\left(\frac{R_A}{R_B}\right)$$

Where $f\left(\frac{R_A}{R_B}\right)$ is the function of the ratio $\frac{R_A}{R_B}$ only.

## 1.4 RESISTANCE TEMPERATURE DETECTOR(RTDs)

Resistance Temperature Detectors (RTDs), as the name implies, are sensors used to measure temperature by correlating the resistance of the RTD element with temperature. Most RTD elements consist of a length of fine coiled wire wrapped around a ceramic or glass core. The element is usually quite fragile, so it is often placed inside a sheathed probe to protect it. The RTD element is made from a pure material whose resistance at various temperatures has been documented. The material has a predictable change in resistance as the temperature changes; the predictable change is used to determine temperature. Some frequently used RTDs are: (i) Platinum (most popular and accurate), (ii) Nickel, (iii) Copper, (iv) Balco (rare), (v) Tungsten (rare) etc. [5]

### 1.4.1 Benefit of using a RTD :

The RTD is one of the most accurate temperature sensors. It not only provides good accuracy, but also provides excellent stability and repeatability. RTDs are relatively immune to electrical noise and therefore well suited for temperature measurement in industrial environments, especially around motors, generators and other high voltage equipment.

| METAL | RESISTIVITY ohm/cmf<br>Cmf = circular mil foot |
|---|---|
| Gold (Au) | 13 |
| Silver (Ag) | 8.8 |
| Copper (Cu) | 9.26 |
| Platinum (Pt) | 59 |
| Tungsten (W) | 30 |
| Nickel (Ni) | 36 |

**Table 1.2 : Resistivities of common RTD materials.[6]**

Because of their lower resistivity, gold and silver are rarely used as RTD elements. Tungsten is reserved for very high temperature applications because of relatively high resistivity. The most common RTD's are made of platinum, nickel, or nickel alloys. The economical nickel derivative wires are used over a limited temperature range. They are quite non-linear and tend to drift with time. For accuracy in measurement, platinum is the obvious choice.

### 1.4.2 Platinum resistance thermometer(PRTs):

Platinum Resistance thermometers are temperature sensors that exploit the predictable change in electrical resistance of platinum with changing temperature. These are being used in place of thermocouples in industrial applications at temperatures below 600 $^{0}$C. At higher temperatures, it becomes difficult to prevent the platinum from being contaminated by impurities from the metal sheath of the thermometer. Platinum resistance thermometer requires a small current to pass through it, to determine its resistance at different temperatures. Platinum has a linear resistance-temperature relationship; we can use this method to find the resistance at different temperatures.

Platinum Resistance thermometer consists of a fine platinum wire (platinum coil) wound in a non-inductive way on a mica frame M (Figure 3.3). The ends of this wire are soldered to points A and C from which two thick leads run along the length of the glass tube (that encloses the set up) and are connected to two terminals (P, P) fixed on the cap of the tube. These are the platinum wire leads**.** Also, by the side of these leads, another set of leads run parallel and are connected to the terminals (C, C) fixed on the cap of the tube. These are called compensating leads and are joined together inside the glass tube. The compensating leads and the platinum wire are

separated from each other by mica or porcelain separators (D, D). The electrical resistance of the (P, P) leads is same as that of the (C, C) leads.[7]

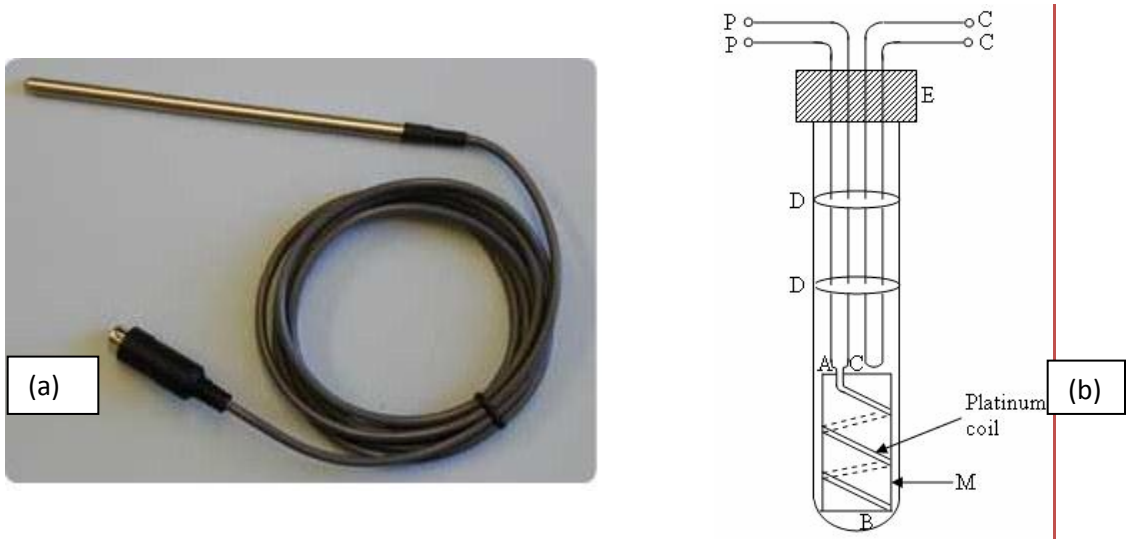


**Fig 1.7: Platinum resistance thermometer (a) Pt-100 probe (b) its schematic representation**.[7]

The most common type (Pt-100) has a resistance of 100 ohms at 0 °C and 138.4 ohms at 100 °C. There are also Pt-1000 sensors that have a resistance of 1000 ohms at 0 °C. The linearization equation of its temperature dependence is:

$$R_t = R_0 * (1 + A* t + B*t^2 + C*(t-100)* t^3)$$

Where,

$R_t$ is the resistance at temperature $t$,

$R_0$ is the resistance at 0 °C,

$A$= 3.9083x$10^{-3}$,

$B$ = -5.775 x$10^{-7}$,

$C$ = -4.183 x$10^{-12}$ (below 0 °C), or

$C$ = 0 (above 0 °C).

For a Pt-100 sensor, a 1 °C temperature change will cause a 0.384 ohm change in resistance, so even a small error in measurement of the resistance can cause a large error in the measurement of the temperature.[8]

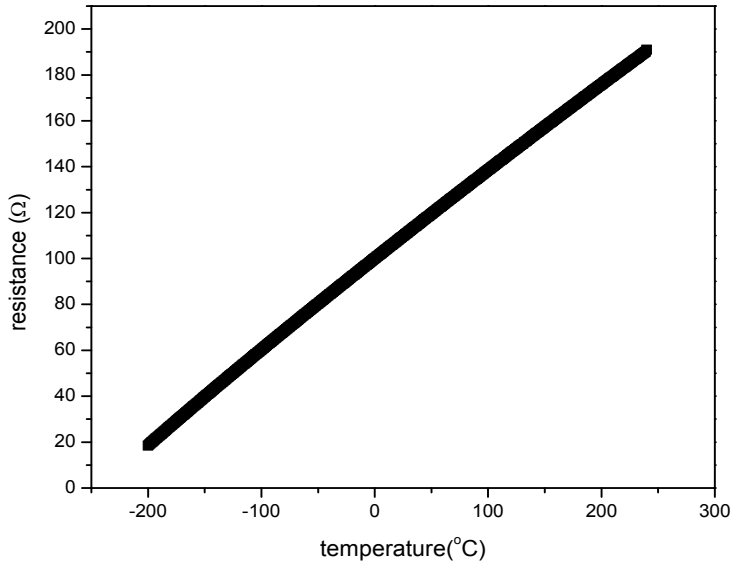


Fig 1.8: plot of resistance vs. temperature of Pt-100 sensor.[9]

## 1.5 THERMOCOUPLE

Thermocouples are the most commonly used temperature measuring device in elevated temperature thermal analysis. The assembly of two different metals joined at their ends to have two junctions in a circuit is called a thermocouple. This phenomenon is known as thermo-electric effect as electricity has been produced from heat. The current thus produced is called thermo-electric current. The thermocouple produces a voltage related to a temperature difference. Thermocouples are a widely used type of temperature sensor for measurement and can also be used to convert heat into electric power. They are inexpensive and interchangeable and can measure a wide range of temperatures. The main limitation is accuracy, system errors of less than one degree Celsius (C) is difficult to achieve.

### 1.5.1 Thermoelectric effect :

A thermoelectric device creates a voltage when there is different temperature on each side. Conversely when a voltage is applied to it, it creates a temperature difference. The thermoelectric

effect encompasses three separately identified effects- the Seebeck effect, the Peltier effect and the Thomson effect.

### 1. Seebeck effect :

A temperature difference between two points in a conductor or a semiconductor results in a voltage difference between these two points. This phenomenon is called seebeck effect. The magnitude and the direction of thermo-emf developed in a thermocouple depend upon the nature of metals forming the thermocouple and the differences in temperature of the two junctions. The seeback effect is reversible i.e. if the hot and the cold junctions are interchanged the direction of thermoelectric current is reversed.

Seeback series is listed in the box below.

Bismuth → Constant → Nickel → Platinum → Mercury → Aluminium →
Lead → Silver → Gold → Copper → Zinc → Iron → Nichrome → Antimony

When any two of these metals form a thermocouple, current flows through the hot junction from a metal occurring earlier to a metal occurring later in the series. For a given differences of temperature of two junctions the larger is the gap in seeback series between the metals forming the thermocouple, the greater will be the thermo-emf generated.

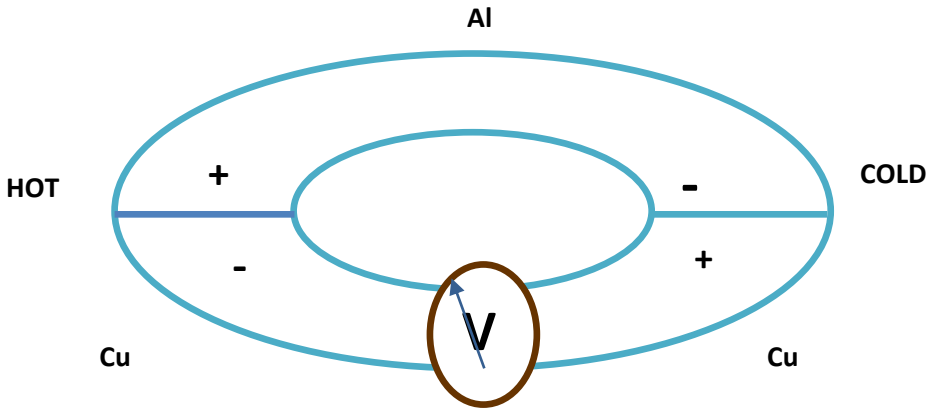


**Fig 1.9: Al-Cu Thermocouple for Seebeck effect**

The electron-density (no. of electrons per unit volume) of a conductor depends on the material of the conductor. When two different metals are brought into contact at the junction, the free electrons tends to diffuse from the metal with greater free electron density to the other with lower free electron density. Due to this diffusion, a potential difference developed at the junction of the two metals called contact-potential. When both the junctions are at the same temperature, the contact potentials at the two junctions will be the same. Hence no current flows in the thermocouple. But if one junction is heated up, the rate of diffusion of free electrons at that junction will change, which results in difference in the contact potential of the two junctions called thermo-emf.

$$V_{thermo-emf} = V_{hot} - V_{cold}$$

**Effect of temperature-**When the two junctions of the thermocouple are at the same temperature galvanometer shows no deflection i.e. thermo-emf is zero. As the temperature of the hot junction increases keeping the cold junction at constant temperature, the thermo-emf increases with increase in temperature until it becomes maximum at certain temperature.

The temperature of hot junction at which the thermo-emf in a thermocouple is maximum is called **neutral temperature ($T_n$).**When the junction is heated beyond $T_n$, thermo-emf starts decreasing.

Neutral temperature ($T_n$) is

- constant for a thermocouple
- depends upon the material of the material of a thermocouple and
- is independent of temperature of cold junction.

At another particular temperature of hot junction the thermo-emf becomes zero and on further heating, the direction of thermo-emf is reversed. The temperature of the hot junction at which the thermo-emf of the thermocouple becomes zero and just beyond which it reverses its direction is called **temperature of inversion ($T_i$).**

Temperature of inversion ($T_i$) depends upon

- the temperature of cold junction and
- on the material of the thermocouple.

$$T_n = \frac{(T_i + T_0)}{2}$$

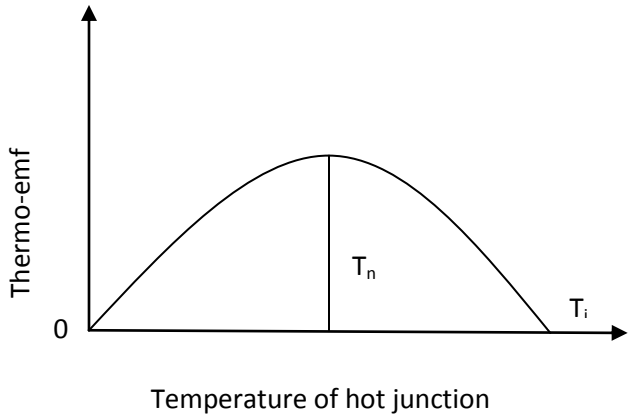


**Fig 1.10: Thermo-emf Vs Temperature of a thermocouple.**

**2. Peltier Effect :**

If a current is passed through a junction of two different metals, the heat is either evolved or absorbed at that junction. This effect is known as Peltier effect. The amount of heat absorbed or evolved at a junction is proportional to the quantity of charge crossing that junction.

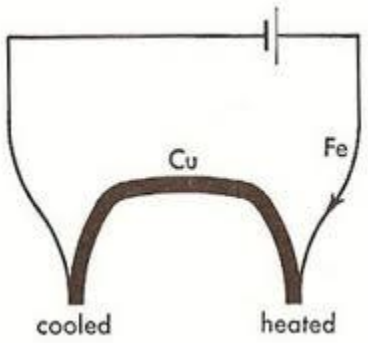


**Fig 1.11: Thermoelectric junction for peltier effect**

If the direction of current is reversed the heating effect at the junction is also reversed. So, peltier effect is reversible effect. It is also complementary to Seebeck effect. Peltier heat is evolved at a

junction of a thermocouple which is kept cold for seebeck effect and the peltier heat is absorbed at a junction of thermocouple which is kept hot for seebeck effect.

**Peltier coefficient-** Amount of heat energy absorbed or evolved at a junction of two different metals when one coulomb of charge passes through that junction.

$$\Pi = \frac{Peltier\ heat}{Charge\ flowing} \text{ (J/C)}$$

Peltier coefficient depends upon

- nature of the two metals forming the junction and
- Temperature of the junction.

**3. Thomson's Effect :**

If two parts of a single conductor are maintained at different temperature, an emf is developed between them. The emf so produced is called Thomson emf. It is the absorption or evolution of heat in excess of joule heat when current is passed through an unequally heated conductor. Thomson effect is reversible effect.

Some substance in which when current flows from hot end to cold end i.e. from higher potential to lower potential, the energy is evolved whereas when current is flowing from cold end to hot end of the rod i.e. from lower potential to higher potential, heat is absorbed , the Thomson effect is positive e.g. Copper, Silver, Zinc, Antimony, etc.

There are some other substances like Iron, Cobalt, Platinum, Bismuth, etc. for which Thomson effect is negative, i.e. heat is absorbed when current is passed from hot to cold end and heat is evolved when current is passed from cold end to hot end of the rod.

In lead (Pb), the Thomson effect is nil i.e. no heat is evolved or absorbed when current is passed through an unequally heated lead.[10]

**Thomson coefficient-**

Amount of heat energy evolved or absorbed between the two points of a conductor maintained at a unit temperature difference when unit current is passed through the conductor.

$$\sigma = \frac{dV}{dT}$$

In a thermocouple,

Seebeck emf = Peltier emf + Thomson emf

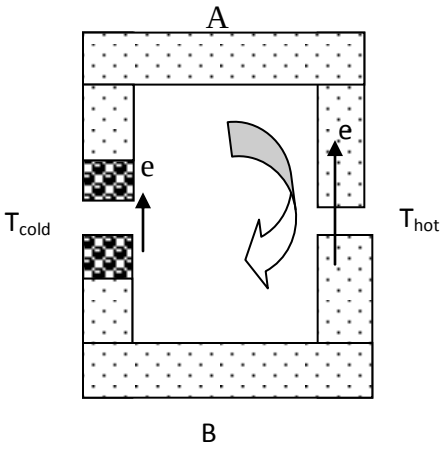


**Fig 1.12: free electron model of thermocouple behavior**

### 1.5.2 Laws of Thermocouple:

- **Law of homogenous material**- A thermoelectric current cannot be sustained in a circuit of a single homogeneous material by the application of heat alone, regardless of how it might vary in cross section.
- **Law of intermediate material**- The algebraic sum of the thermoelectric forces in a circuit composed of any number of dissimilar materials is zero if all of the junctions are at a uniform temperature. So If a third metal is inserted in either wire and if the two new junctions are at the same temperature, there will be no net voltage generated by the new metal.
- **Law of successive or intermediate temperature**- If two dissimilar homogeneous materials produce thermal emf1 when the junctions are at T1 and T2 and produce thermal

emf2 when the junctions are at T2 and T3 , the emf generated when the junctions are at T1 and T3 will be emf1 + emf2 .[10]

### 1.5.3 Types of Thermocouples :

Certain combinations of alloy form different types of thermocouples. Selection of the combination is driven by cost, availability, convenience, melting point, chemical properties, stability, and output. Different types are best suited for different applications. They are usually selected based on the temperature range and sensitivity needed.

| TYPES | METAL | | STANDARD COLOR CODE | | IDENTIFICATION | | MAX. USEFULL RANGE | |
|---|---|---|---|---|---|---|---|---|
| | POSITIVE | NEGATIVE | POSITIVE | NEGATIVE | MAGNETIC LEAD | STIFFEN LEAD | TEMP($^{O}$C) | Emf (mV) |
| B (oxides) | Pt (30% Rh) | Pt (6% Rh) | Grey | Red | | +ve | 0-1700 | 0-12.4 |
| E (non-magnetic) | Chromel | Constatan | Violet | Red | | | -200 to 900 | -8.8 to 68.8 |
| J | Iron | Constatan | White | Red | +ve | | 0-750 | 0-42.3 |
| N | Nicrosil | Nisil | Orange | Red | | | -270 to 1300 | -4.3 to 47.5 |
| K | Chromel | Allumel | Yellow | Red | -ve | | -200 to 1250 | -6.0 to 50.6 |
| R | Pt (13% Rh) | Pt | Black | Red | | +ve | 0-1450 | 0-16.7 |
| S | Pt (10% Rh) | Pt | Black | Red | | +ve | 0-1450 | 0-15.0 |
| T | Cu | Constatan | Blue | Red | | | -200 to 350 | -5.6 to 17.8 |
| C | W (5% Re) | W (26% Re) | White | Red | | | 0-2320 | 0-38.6 |

**Table 1.3: Types of thermocouple and their properties.[10]**

# CHAPTER 2

## INSTRUMENTATION

This chapter gives the details of design and fabrication of high temperature resistivity setup. The set up involves a controlled furnace and four probe resistance measuring probe station with temperature control and measurement unit. A preliminary investigation was conducted first to study the temperature stability and ramping control on the power supplied to the designed furnace.

## 2.1 Furnace Designing

In able to provide high temperature ambiance to the four probe setup, a furnace is designed which can go to the desirable high temperature. A "wound furnace" was made where a refractory metal wire is wrapped around the alumina tube. For our case Kanthal wire is chosen because it can provide temperature as high as $1000^{o}$C. Length of the wire which gives a resistance of 50 ohms is cut and a coil is made from this wire. The coil so made is wound over the alumina tube. In order to keep the winding intact and firm, an insulating adhesive was applied over the winding.

To make the insulating adhesive, ceramic brick (made up of silicon and aluminium) is crushed to fine powder, which is then mixed with sodium silicate gel to make a paste to be used as cementing material. This paste is then applied over and between the gaps of the coil wound over the alumina tube, to avoid overlapping of the coil. Then the tube assembly (kiln) is left for one week for drying.

The outer body of furnace is made from stainless steel container, commercially available in the local market. Before putting the kiln inside the SS container, a thick layer of ceramic wool is put in the base. On the steel container, three holes are made, one for the control thermocouple which touches the kiln to measure its temperature and two holes for the electrical connection to the coil. All the holes are well insulated using ceramic beads. The heating coil (Kanthal) wound over the alumina was provided three layers of insulation to get the best temperature stability and minimum heat loss. The first layer is the ceramic brick + sodium silicate pasted and dried over the coil. The second layer is the dry ceramic brick powder tightly packed around the alumina tube. Then the last layer of ceramic wool nicely packed after the ceramic brick powder. The

ceramic wool is very light weight and can withstand a temperature up to 1200$^{o}$C. The use of ceramic wool makes the furnace light weight.

The electrical power to the furnace is given via temperature controller. The working details of the temperature controller are shown in the block diagram below. The temperature of the furnace is sensed via K-type thermocouple connected to the ON/OFF controller. This ON/OFF controller cannot control more than 3 amp of current, hence an automatic electromechanical switch is made using Relays capable of carrying 10-15 amp of current. The output of the ON/OFF controller is fed in a step down (220 to 12V) transformer. This transformer is used to control the relay, connected in series with the AC mains and Furnace. However when the relay is ON, full 220V is applied across the furnace coils, which may heat the furnace to overshoot the set temperature. In order to sweep the temperature very slowly, a potential divider arrangement is added between the relay and the furnace. Using the potential divider arrangement, the current in the coil can be controlled for desired sweeping rate and set temperature. It should be noted that potential divider arrangement is necessary not only to control the sweeping rate, but also to set the temperature to desired values with minimum fluctuation.

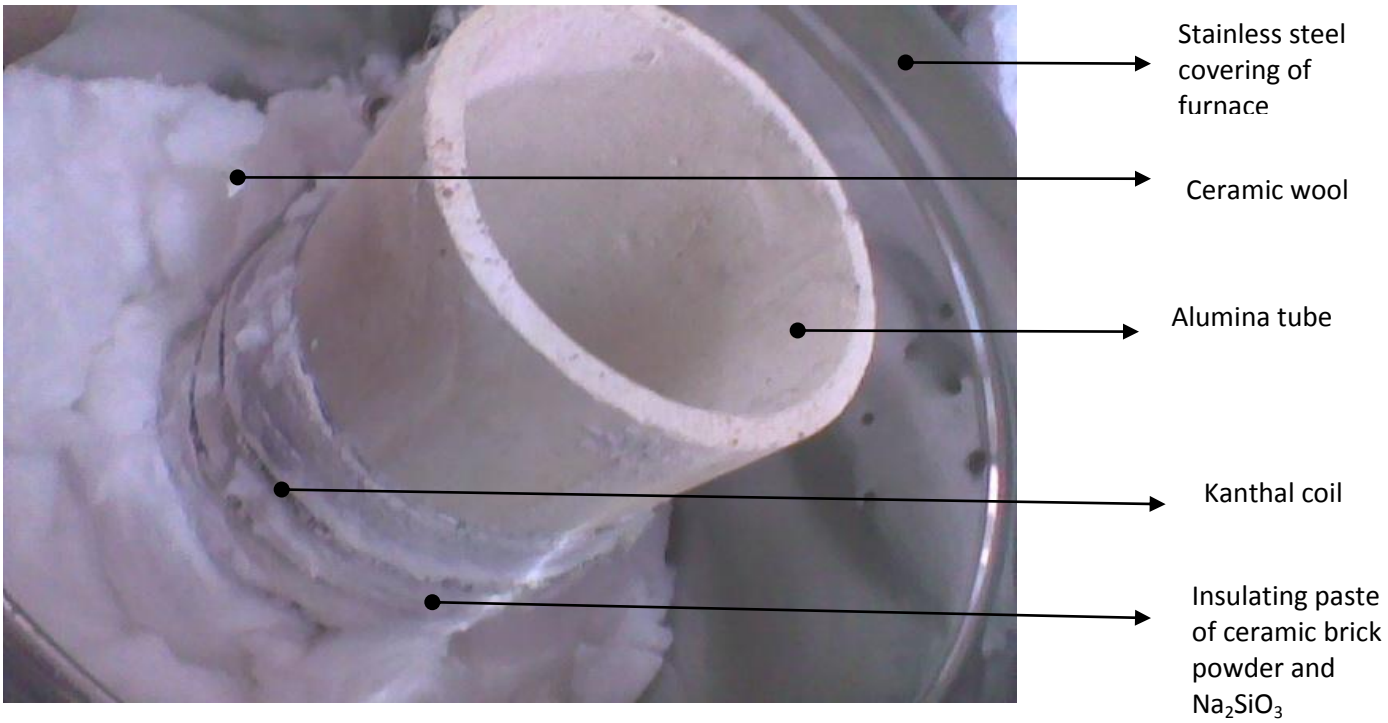


**Fig 2.1: Interior of the furnace.**

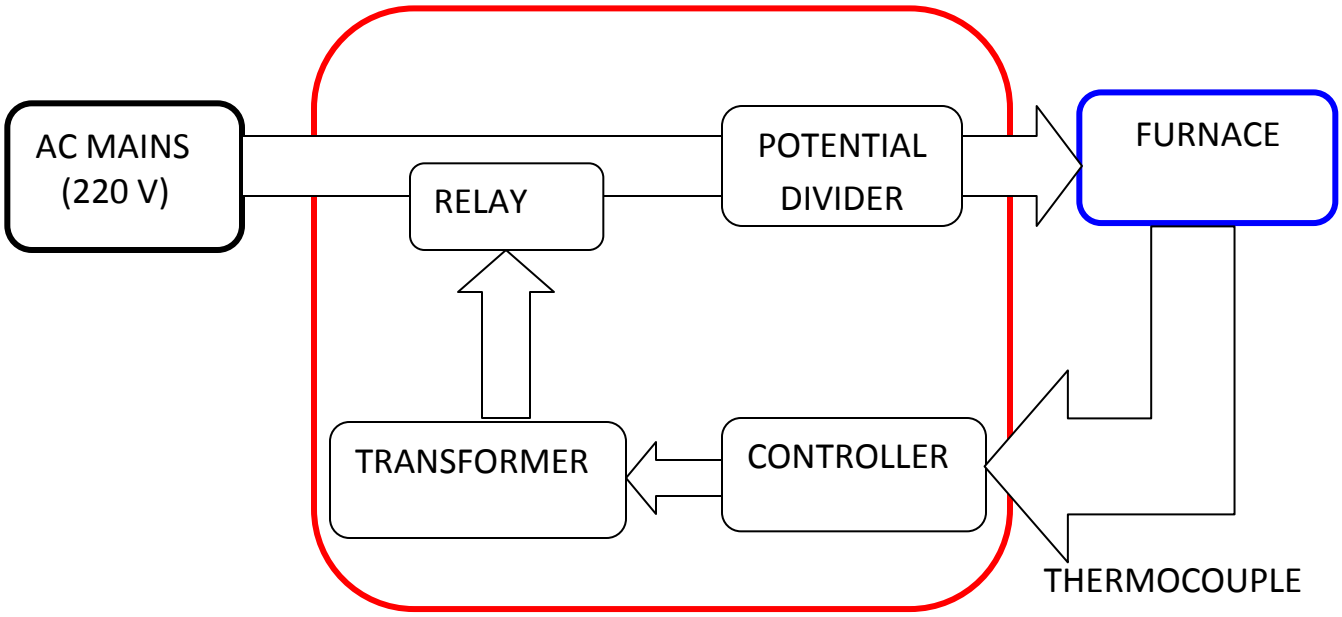


**Fig 2.2: Block diagram of Furnace control**

**AUTOMATIC CONTROL SYSTEM**

1. On-Off Control: Set point temperature is the desired temperature of the furnace at any given time. If the furnace temperature is above the set point, the furnace shut-off. If the furnace temperature is below the set point, the furnace goes to full power. As a result the furnace temperature tends to oscillate about the set point value. As on-off switching fatigues mechanical relay with time , a dead-band is often introduced where by the system does not shut off until the furnace temperature exceed few degree and does not turn on until the furnace temperature drops below the set point by few degrees. The introduction of dead band will increase the amplitude of oscillation but decrease its frequency, preserving the life of the relay.

2. Proportional Control: It eliminates furnace temperature oscillation by applying the correction which is proportional to the deviation from the set point.[12]

PID (Proportional Integral Derivative) control system

Proportional

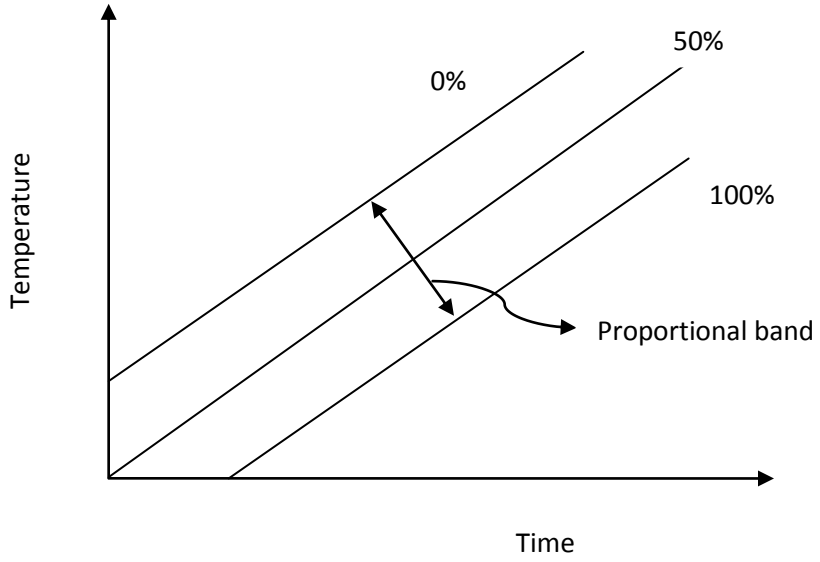


**Fig 2.3: Graph showing the proportional control of PID control system**

A proportional band is assigned so that if the furnace temperature exceeds these outer limits, the system reverts back to on-off control.

If the proportional band is adequately broad, the furnace temperature does not oscillate rather it runs parallel to the set point and if the proportional band is too narrow, the furnace temperature will oscillate as if under on-off control. This elimination of parallel ramping is done by an integral function which continuously sums the difference between furnace and set point temperature as swept through the time.

Integral

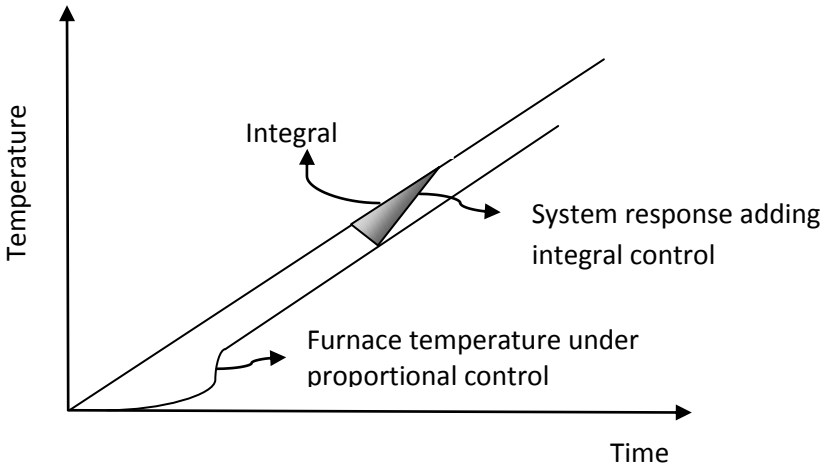


**Fig 2.4 Graph showing the integral control of PID control system.**

This area multiplied by a weighing factor is added to the proportional portion of the control instruction. If the furnace temperature is persistently below the set point, this area continues to accumulate until the furnace temperature is forced up to the set point at which time no additional area is accumulated.

When the furnace temperature lags a desired temperature behind that of set point, the SCR permits more power through and eventually the furnace temperature rise with so much momentum that it overshoots the set point. To minimize overshooting and undershooting effects derivative control may be introduced.

The derivative function strives to keep the slope of the furnace temperature with time the same as that of set point with time.

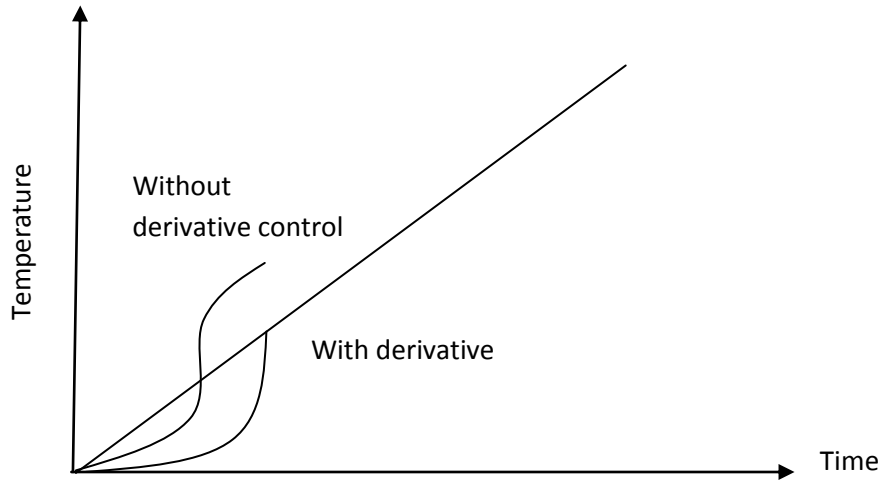


**Fig 2.5: Graph showing derivative control of PID control system**

Derivative control acts as a predictive function, whereby if the temperature is below the set point, but is rising rapidly, it (multiplied by a weighing constant) subtracts power from the control instruction. So that it coincides with set point minimizing overshoot.

PID control system is represented as

$$P = P_0 - U_P(T - T_S) - U_I \int_0^t (T - T_S)dt - U_D(dT/dt - dT_S/dt)$$

Where P=power

$P_0$=arbitrarily assigned starting power

T=furnace temperature

$T_S$=set-point temperature

$U_P$, $U_I$ and $U_D$ are proportionality constant for proportional, integral and derivative respectively.

In the designed system, an on-off temperature controller was used for high temperature measurement. The temperature controller was then calibrated with the increase in the percentage of power supply by every 10 degree rise in temperature from $100^0$ C to $500^0$ C. The figure below shows the calibrated graph of the furnace temperature controller.

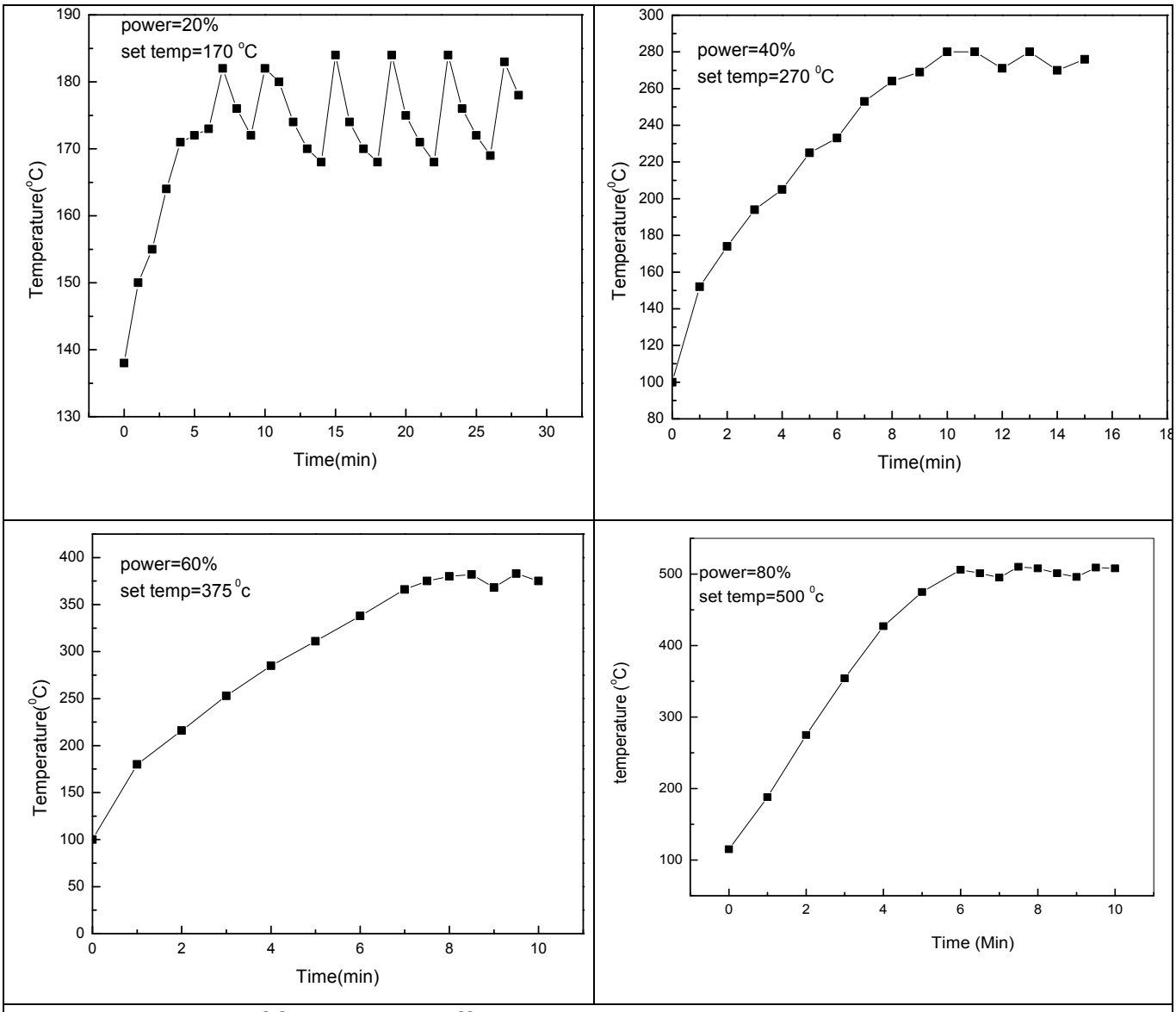


**Fig 2.6 Calibration of furnace with different power percentage and set point temperature.**


**Fig 2.7 : Image of furnace with temperature controller.**

[1] Furnace; [2] Porcelain connectors for electrical connection; [3] thermocouple; [4] Temperature controller; [5] Power regulator; [6] Digital panel; [7] Set point adjust

## 2.2 Four Probe Assembly

The actual working four probe setup is shown in the fig 2.8. The assembly is supported on three stainless steel (SS) studs. Two copper disks of width 8mm & diameter 8cm is cut from a solid cylindrical copper rod. Copper is chosen for this purpose, because of good thermal conductivity to the sample. An aluminium sheet of dimension 11 x 11 cm was cut from a large sheet. Three 4mm holes are drilled over all the three metal plates in a tripod like manner so that studs can be inserted which act as a supporting stand. In one of the copper disk (middle) and aluminium sheet, a hole of 8.2mm was drilled at the center so that ceramic beads containing four copper wires can be inserted. Near the central hole, another hole of 6.5mm is drilled to insert Pt-100 sensor, resting over the bottom copper base. In the aluminium plate 8.5mm hole was drilled in the same line as in the copper disk where 6.5mm hole is placed. The three metal plates are assembled together at a distance of 6.5cm from each other with the help of three studs and nuts. Four equal sized copper wires of length 23cm was cut and sharpened at the ends. These four copper wires are insulated by inserting them inside four–holed ceramic beads. This assembly is inserted in the central hole of the four probe system.

Out of the four copper wires of the four probe, two were connected to Keithley nanovoltmeter for voltage measurement and other two were connected to Keithley current source which supplies constant dc current to the probes. Pt-100 sensor was connected with a digital ohmmeter for the measurement of resistance with the variation of temperature. Keithley nanovoltmeter and Keithley current source was interfaced with the computer using Labview software for the resistance measurement.

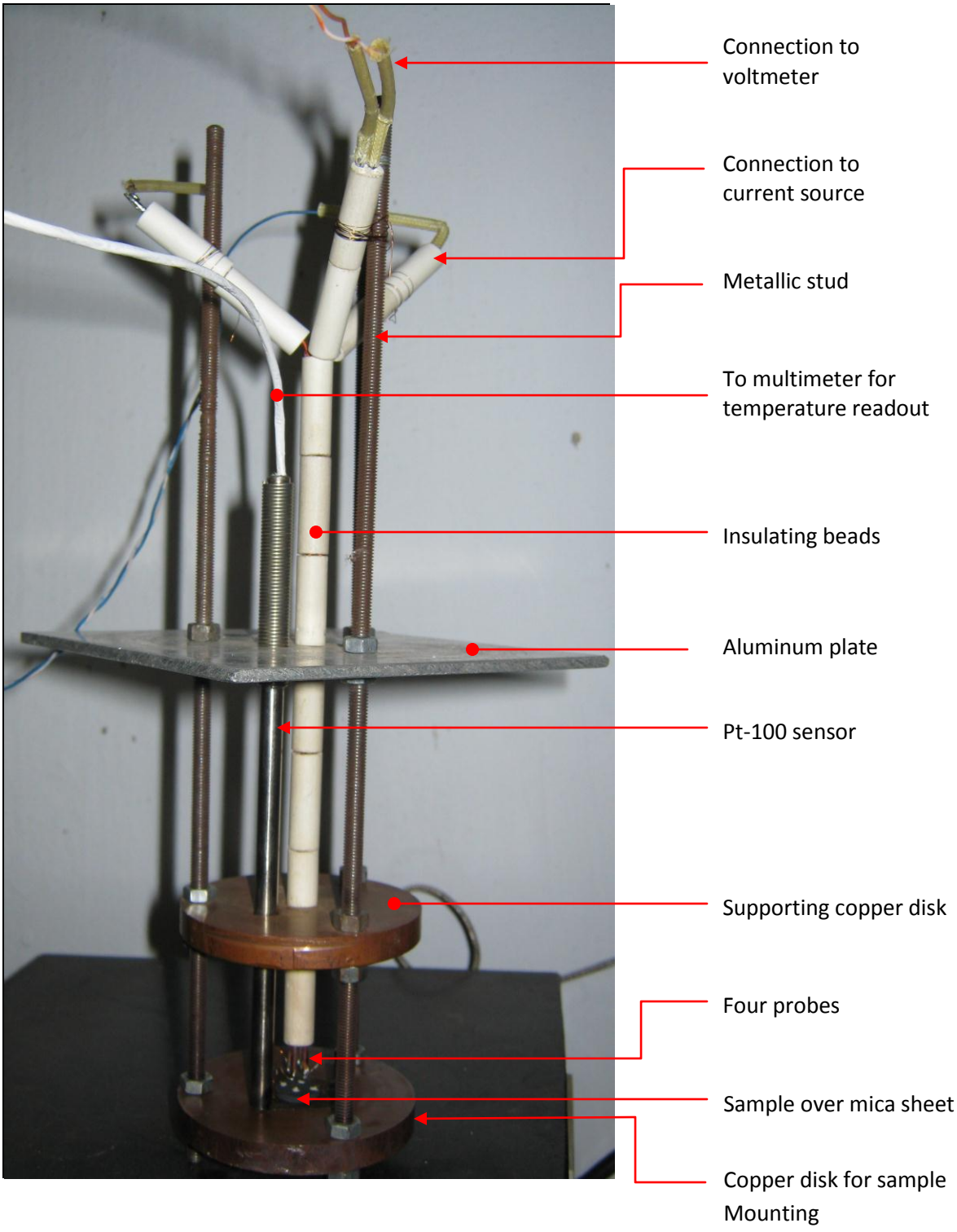


**2.8: Image of four probe assembly.**

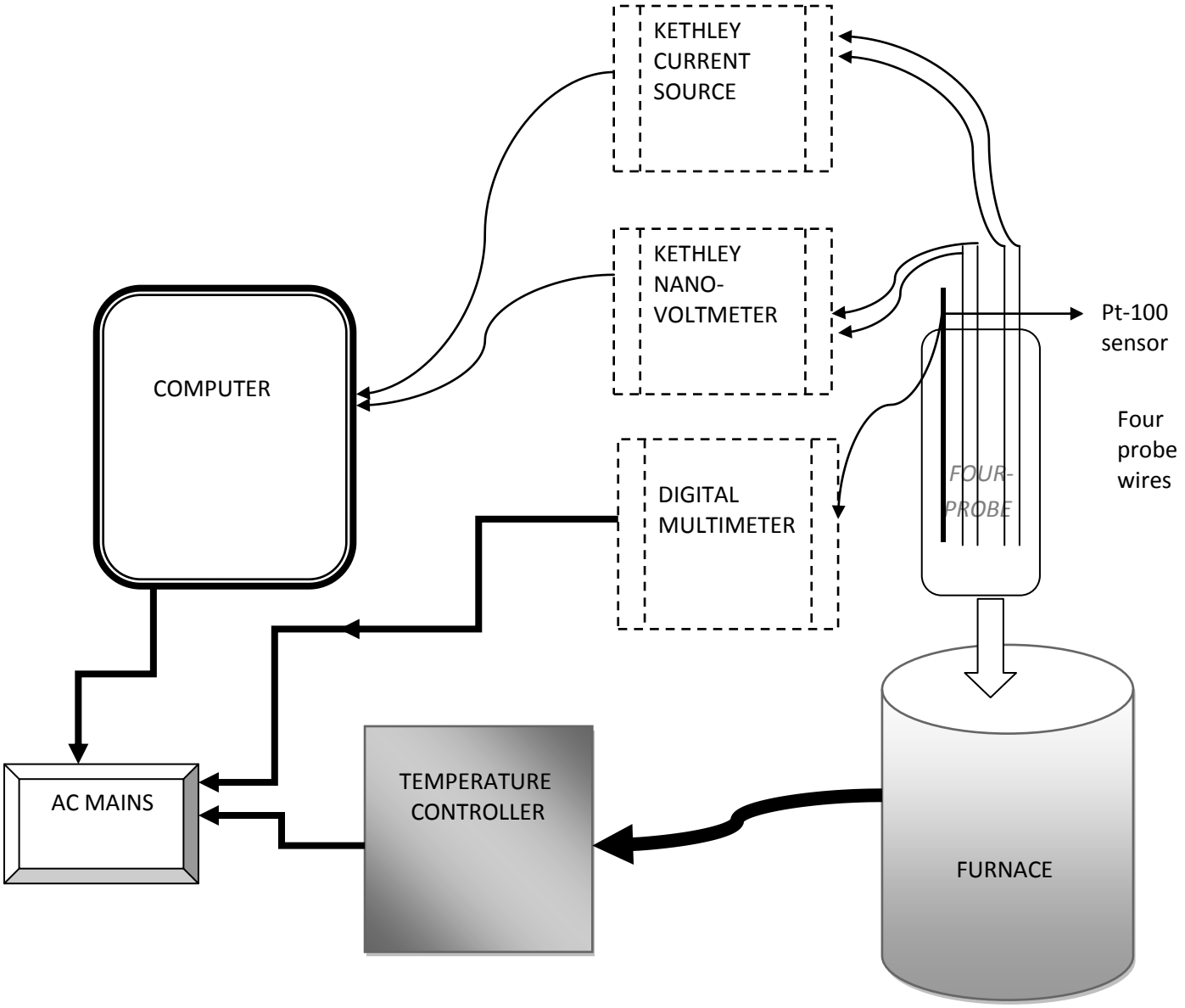


**Fig 2.9: Block diagram of the designed resistivity set up.**

# CHAPTER 3

# SAMPLE PREPARATION

## 3.1 CHOICE OF SAMPLE

Recently ceramic magnetic oxide nanoparticles are of much interest because of their unique magnetic, electronic and optical properties. Cobalt ferrite ($CoFe_2O_4$) is one such hard magnetic material with moderate magnetisation. It has high coercivity and good chemical and physical stability [13]. It has high electrical resistance with low eddy current loss. It has broad applications in permanent magnets, drug delivery, microwave devices, hydrogen production and switch memory devices. It is a good dielectric material and has applications in technology ranging from microwave and radio frequency [14].

## 3.2 APPLICATIONS OF COBALT FERRITE

a) **Biomedical applications**:

Ferrites are biocompatible, so they have a large application in magnetic target and drug delivery, magnetic fluid i.e. Ferro fluid, hyperthermia in cancer treatment etc.

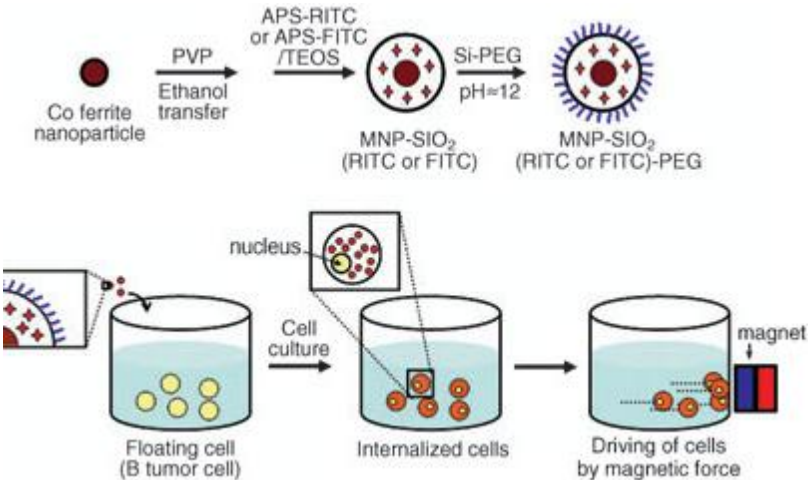


**Fig3.1: Schematic illustration of removal cancer cell by application of external magnetic field on magnetic nanoparticle capped with $SiO_2$ [15].**

b) **Hydrogen production**:

Hydrogen is produced by oxidation and reduction reaction of water. The electrolyte used is NaOH and the two electrodes used are platinum electrode for $H_2$ production and cobalt ferrite film for $H_2O$ oxidation [16].

In this hydrogen production system, silicon solar cell and electrolytic cell are used as active components. For water electrolysis, silicon solar cell provides biasing current to the cathode-anode electrode assembly in an electrolytic cell.
The water electrolysis is manifested in three steps. The incident solar energy generates electron-hole pairs due to silicon solar cell, in a first step. In a second step, these electron-hole pairs flow through the cathode-anode electrolyte assembly followed by water electrolysis in a third step,

Energy (solar) + Si solar cell $\rightarrow 4e^- + 4H^+$ (1)

At cathode: $4H_2O+4e^- \rightarrow 2H_2 + 4OH^- + 4H^+$ (2)

At anode: $4OH^- + 4H^+ \rightarrow O_2 + 2H_2O+4e^-$. (3)

c) **Magnetic Stress sensor application**:

Metal bonded cobalt ferrite composites are used in magnetoelastic stress sensors, due to their large magnetostriction and high sensitivity of magnetization to stress. They have large strain derivatives and high sensitivity of magnetization to applied stress. These magnetic property changes can be detected remotely, e.g., by measuring magnetic field near the sensor surface using a Hall effect device. Magneto-elastic materials offer realistic prospects for development of contactless sensors for use in stress and torque applications [17].

d) **Batteries**:

Cobalt ferrite is used in the anode of lithium ion batteries [18]. The electrochemical reaction mechanism of CoFe2O4 is given as

$CoFe_2O_4 + 8Li \longrightarrow Co + 2Fe + 4Li_2O$

It is an irreversible process which leads to the formation of metallic cobalt, iron and lithium oxide. The following reversible oxidation/reduction processes then take place in the subsequent charge/discharge cycles:

$$Co + 2Fe + 4Li_2O \rightleftharpoons CoO + Fe_2O_3 + 8Li$$

Both reversible redox reactions of $Co^{II} \longleftrightarrow Co^0$ and $Fe^{III} \longleftrightarrow Fe^0$ contribute to the specific capacity of $CoFe_2O_4$ film electrode.

e) **Microwave application of soft ferrite**:

Microwave devices are used in signal processing, radar detection, communication and instrumentation. [19]

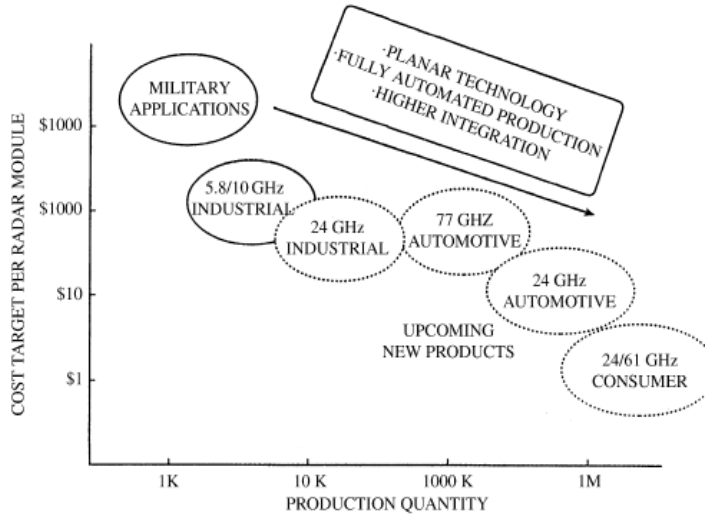


**Fig 3.2: Microwave sensor products [19]**

## 3.3 SAMPLE SYNTHESIS

Conventional techniques for preparation of cobalt ferrite includes

- Sol gel method [14].
- Electrostatic spray method [16].
- Pulse laser deposition [18].
- Microwave route [20].

- Low temperature- auto combustion method [21].
- Magnetron sputtering [22].
- Co-precipitation method [23].
- Hydrothermal method [24].

Out of all these methods, sol-gel method is implemented for the preparation of cobalt ferrite. The precursors used were cobalt nitrate ($Co(NO_3)_2.6H_2O$), iron nitrate ($Fe(NO_3)_3.9H_2O$) and Glycine ($CH_2NH_2COOH$) as fuel. These materials are dissolved in deionised water to obtain the precursor solution. This solution is then concentrated in a glass beaker using magnetic stirrer until excess of water evaporates. Glycine to nitrate ratio is maintained at 1:1 i.e. if 0.02 moles of cobalt nitrate and iron nitrate is taken then 0.04 mole of glycine is taken. The reaction involved in the sample preparation is given as

$$18Fe(NO_3)_3+9Co(NO_3)_2+32NH_2CH_2COOH+54O_2 \longrightarrow 9CoFe_2O_4+ 16N_2+72NO_2+ 34CO_2+ 80H_2O$$

The quantities such as conductivity and resistivity are greatly influenced by porosity, grain size and microstructure of the sample.

The flow chart for the preparation of cobalt ferrite is given below.

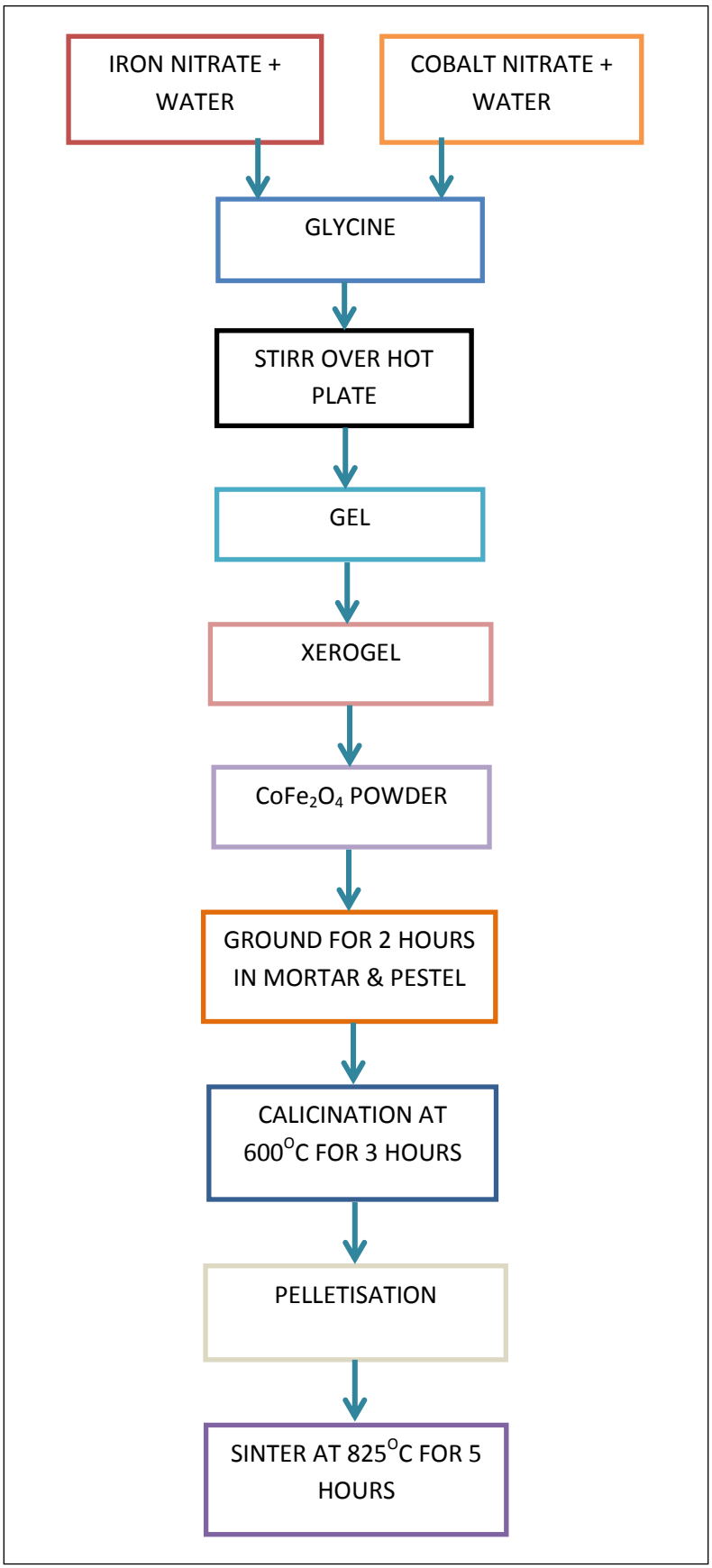


**Fig 3.3: Flow chart for preparation of CFO**

# CHAPTER 4

## RESULTS AND DISCUSSION

### 4.1 Sample characterization

**X-ray diffraction analysis**:

The X-ray diffraction technique is used to determine the atomic arrangements (i.e., crystal structure) of the materials because the interplanar spacing (d-spacing) of the diffracting planes is of the order of X-ray wavelength. For a crystal of given d-spacing and wavelength λ, the various orders n of reflection occurs only at the precise values of angle θ which satisfies the Bragg condition $2d \sin\theta = n\lambda$. The determination of interplanar spacing, lattice parameters etc. provides an important basis in understanding of various properties of materials

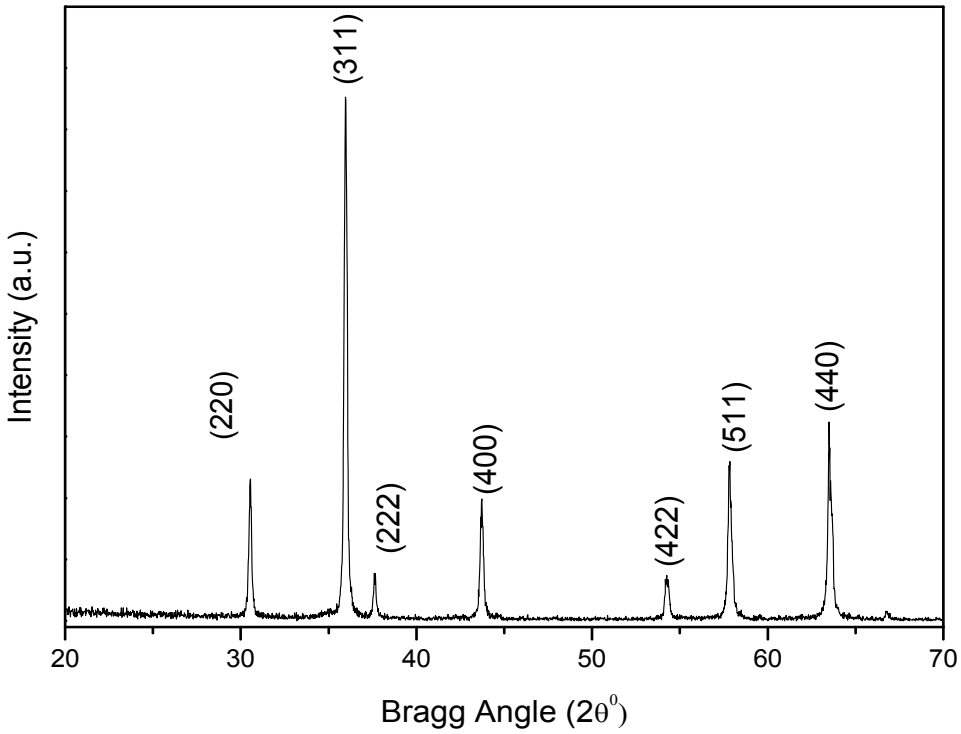


**Fig 4.1: X-ray diffraction pattern of CFO**

Figure 1 shows the XRD pattern of CFO carried out at room temperature. The sharp and single diffraction peaks, which are different from those of the precursors, confirm the formation of single phase compound of CFO. The observed XRD pattern matched with the standard XRD

pattern of CFO ( ). The peak position (2θ), full width at half maximum (FWHM), and intensity of each peak are calculated using a commercially available software (PEAK FIT) [25]. Indexing of XRD patterns is carried out with the help of software (POWD) [26] by least-squares method using diffraction angle (2θ) and intensity value of each peak as input parameter. The best agreement between the observed interplanar-spacing and Bragg angles with the calculated one found for the cubic crystal structure. The least squared refined lattice parameters are found to be a=8.391 (49) $A^0$ and the unit cell volume is 84.58 (49) $(A^0)^3$ (the standard deviations are in parenthesis).

**4.2 Williamson-Hall method:**

The broadening of X-ray diffraction peaks is assumed to be mainly due to small crystallite size and strain of the material. The Williamson-Hall method was used to find out the crystallite size and rms value of strain of CFO sample using the following equation:

$$\beta\cos\theta = 4\varepsilon\sin\theta + \frac{\lambda}{D}$$

where, β is the FWHM of XRD peaks , D is crystallite size and ε is the rms strain respectively. By plotting βcosθ vs. 4sinθ, strain can be calculated from the slope and crystallite size can be calculated from the intercept of the ordinate.

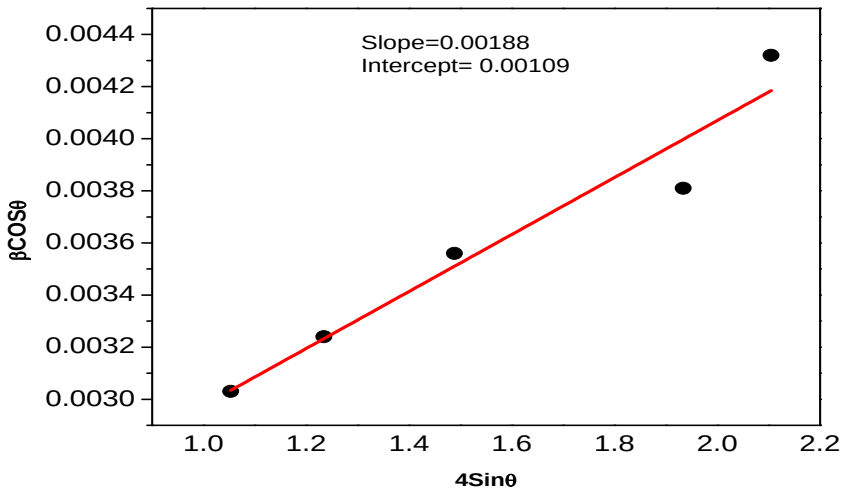


**Fig. 4.2 Williamson Hall plot of CFO.**

The Williamson–Hall plot of CFO is shown in figure 4.2. From the graph, the crystallite size (D) is found to be 141.35 nm and strain to be 0.00188.

### 4.3 Resistivity Measurement:

The dc resistivity of the CFO sample is measured by four probe set up using Keithley nano-voltmeter 2182 and Keithley current source 6221. The measurement is carried out in a temperature range of 300K to 550K in a self-made furnace. Electrical contacts to the sample are made via conducting silver epoxy, in accordance with the Van-der Pauw method. A constant current is applied to two consecutive probes and the voltages at different temperatures are measured at the other two probes. All the data except, Pt100 resistance are collected in a PC via Lab View programming. The values of Pt100 resistance is noted down manually, as the multimeter had no option of interfacing. From the obtained resistances, resistivity can be calculated as: $\rho = \pi R d / \ln 2$, where, ρ is the resistivity, R is the measured resistance, and d is the sample thickness.

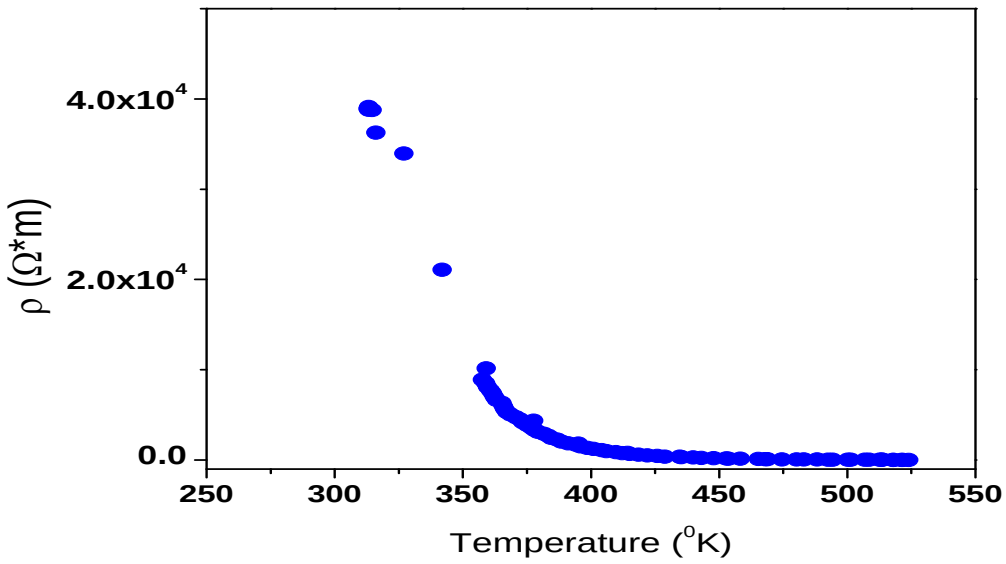


**Fig 4.3: Temperature dependent resistivity of CFO.**

Figure 4.3 shows the dependent resistivity of CFO. From the graphs it has been observed that the resistivity of CFO decreases with the increase in temperature. The decrease in the resistivity is

found to be more prominent at low temperatures as compared to high temperature. This pattern of variation of resistivity suggests that the electrical behaviour of CFO is like a semiconductor.

### 4.4 Calculation of activation Energy:

Fig. 4.4 shows the variation of $\sigma_{dc}$ with $10^3/T$ of CFO sample. It is observed that the dc conductivity increases with increase in temperature. This graph is useful to calculate the activation energy of the material.

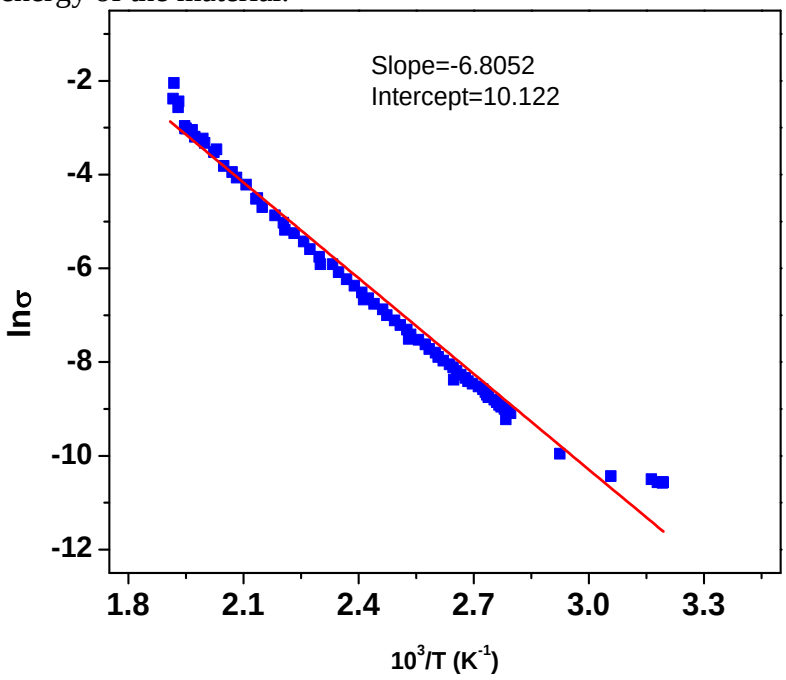


**Fig 4.4: Variation of $\sigma_{dc}$ with inverse of temperature of CFO.**

This plot is more or less a straight line and can be explained by Arrhenius type relation: $\sigma_{dc} = \sigma_0 \exp(-E_a/K_BT)$, where $\sigma_0$ pre-exponential term, $E_a$ is the activation energy, $k_B$ is the Boltzmann constant and T is the temperature in degree kelvin. The solid line represents the fitting of the experimental data to the Arrrhenius equation. There is more or less close agreement between the experimental value (the symbols) and the fitted data (solid line). The activation energy calculated from the slope is found out to be 0.586 eV. Activation energy of a sample is the energy that must be supplied for the electrical conduction (i.e., the minimum energy required to start electrical conduction for the conducting species).

# CHAPTER 5

## CONCLUSION AND FUTURE SCOPE OF RESEARCH

### 5.1: CONCLUSION

A furnace which can withstand about $600^0$C temperature is successfully developed which involves a four probe assembly, sample holder, temperature control and measurement unit. The designed furnace is calibrated at different power percentage and the graph at higher temperature is found to be almost linear with time. The synthesis of cobalt ferrite nanoparticle is done by sol-gel auto combustion method. XRD analysis confirms the formation of this ferrite structure in single phase. The temperature dependence of resistivity for cobalt ferrite is measured in the designed high temperature four probe setup. The dc resistivity of cobalt ferrite was studied extensively.

Based on results obtained, the following conclusions may be drawn.

- From the XRD analysis, it was found that cobalt ferrite has cubic structure.
- The lattice parameters are calculated using standard software POWD and it was found to be $8.391A^0$.
- The temperature vs. resistivity graph suggests that cobalt ferrite is a semiconductor.
- Williamson hall method is used to determine crystallite size and strain which is found to be 141.35 nm and 0.00188 respectively.
- Activation energy is calculated from the resistivity data, using Arrhenius equation and is found to be 0.586 eV.

### 5.2 Future work

- We have measured the resistivity of the sample from room temperature ($30^0$C) to $280^0$C by heating and cooling. For better analysis of electrical properties, resistivity below room temperature can be studied using liquid nitrogen as cooling agent.

- In the present configuration, we have used silver epoxy for electrical connection to sample. This limits the resistivity measurement at higher temperatures. To increase the temperature range of measurement, pressure contacts can be made on the wires of the four probes that touch the sample surface perfectly throughout the experiment.
- Our setup has provision for measuring only resistivity of a given sample. The set up may be improved further for simultaneously measurements of other physical properties such as dielectric constant, thermal conductivity, photoconductivity, etc.

# APPENDIX

This project is a collaborative work of me and my friend Sushree Rosyla Barpanda. Together we have prepared two ceramic oxide ( LSMO and CFO). LSMO ($La_{0.66}Sr_{0.33}MnO_3$) is synthesis using sol gel method. It was then characterised by XRD. Its resistivity measurements were taken using the same resistivity setup. The details about LSMO preparation and characterisation can be found in the thesis of Sushree Rosyla Barpanda. The results of LSMO are summarised below.

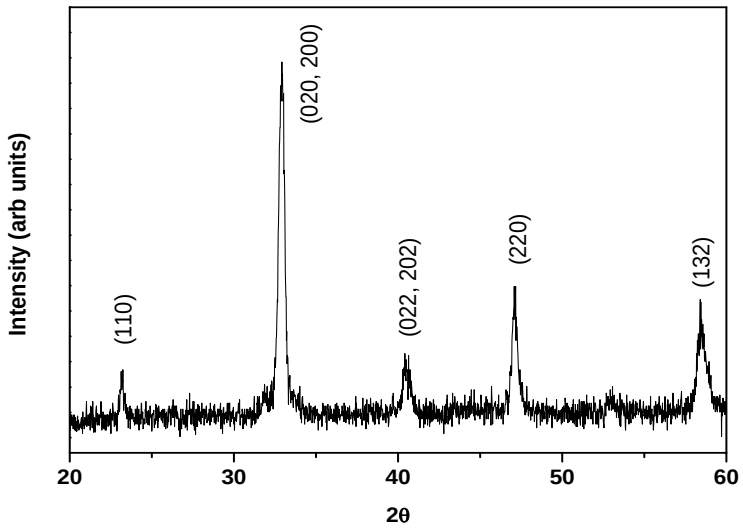


**Fig 1: X Ray Diffraction pattern of LSMO.**

From XRD analysis the crystal structure was found to be orthorhombic. The lattice parameter calculated from POWD software were found to be a=3.8550(17) $A^0$, b=3.8367(17) $A^0$ and c=3.8794(17) $A^0$ and the unit cell volume is 57.378(17) $(A^0)^3$ (the standard deviation are in parenthesis).

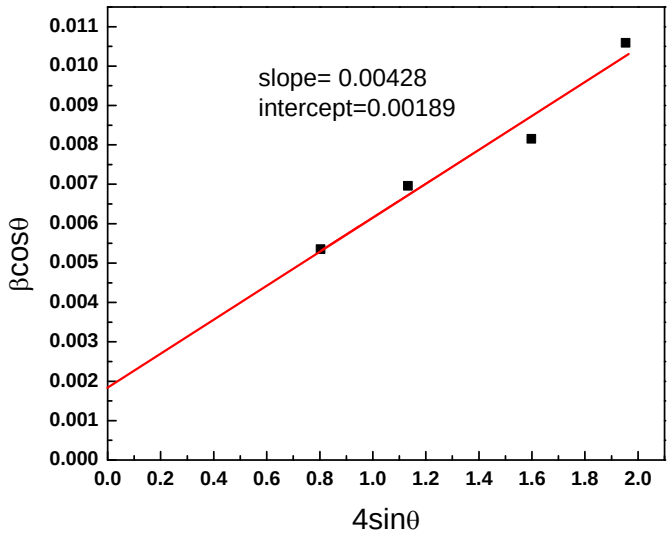


**Fig 2: Williamson Hall plot of LSMO.**

The crystallite size from Williamson hall equation was found to be 81.5 nm and strain was found to be 0.00428.

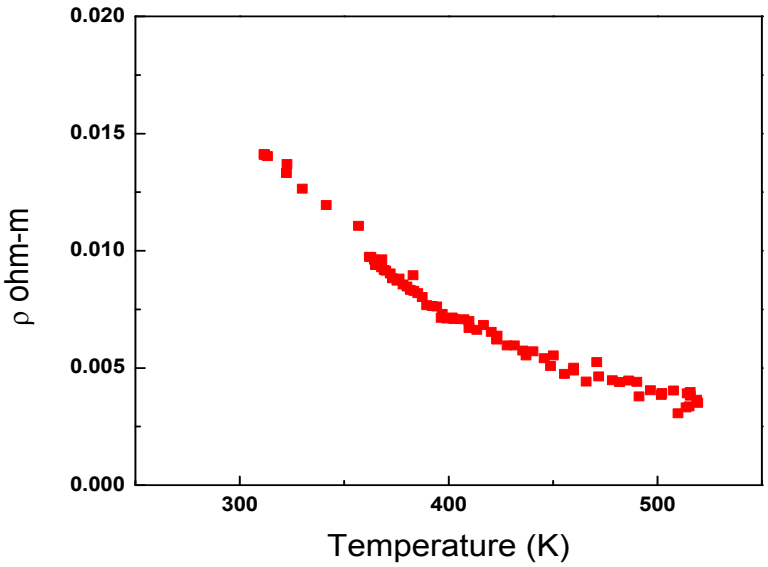


**Fig 3: Resistivity plot of LSMO**

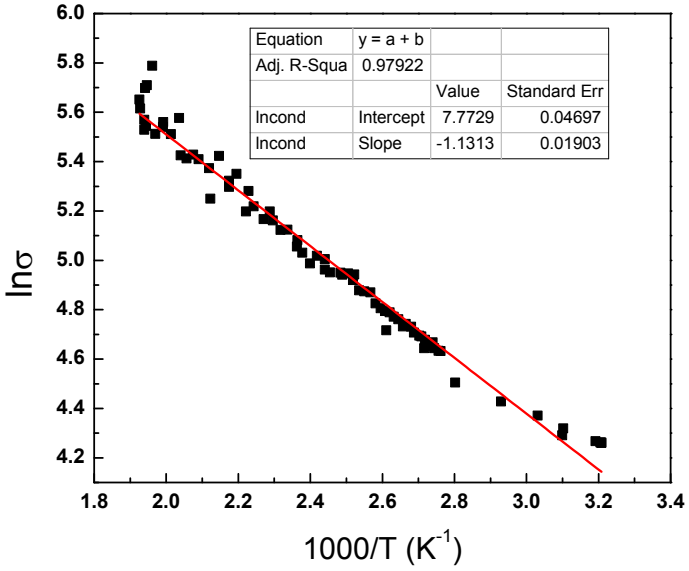


**Fig 4: Variation of $\sigma_{dc}$ with inverse of temperature of CFO.**

From figure 4, activation energy can be calculated from the slope which is found out to be 0.09758 eV.

# REFERENCES


[1] www.wikipedia.org/wiki/resistance

[2] www.teachers.web.cern.ch

[3] www.earthscience.unimelb.edu.au

[4] www.spiff.rit.edu

[5] www.omega.com

[6] www.omega.com/temperature/z/pdf/z033-03j.pdf

[7] www.maitreyi.du.ac.in

[8] www.picotech.com/applications/pt-100.html

[9] http://www.intech.co.nz/products/temperature/typert.html

[10] K.L. Gombler, K.L. Gogia; Fundamental Physics

[11] www.wikipedia.org/thermocouple

[12] Robert F. Speyer, Thermal analysis of materials.

[13] B.G Toksha et al.,Structural investigations and magnetic properties of cobalt ferrite nanoparticles by sol gel auto combustion method; Solid state communication147(2008)479-483.

[14] I.H. Gul, A. Maqsood, Structural magnetic and electrical properties of cobalt ferrite prepared by the sol-gel route, Journal of Alloys and Compounds 465(2008)227-231.

[15] Tae-JongYoon et al., Multifunctional Nanoparticles Possessing A “Magnetic Motor Effect” for drug or gene delivery, Angew. Chem. Int. Ed44 (2005)1068-1071.

[16] Rajendra S. Gaikwad et al., Cobalt ferrite nanocrystallites for sustainable hydrogen production application, International Journal of Electrochemistry vol(2011), article id 729141

[17] J.A. Paulsen et al. , manganese substituted Cobalt ferrite magnetostrictive materials for magnetic stress sensor application, Journal of applied physics97(2005),044502

[18] Yan-Qui Chu et al., Cobalt ferrite thin film as anode material for lithium ion batteries, Electrochemical Acta49(2004)4915-4921.

[19] Martha Pardhavi-Hovarth, Microwave application of soft ferrites, journal of magnetic materials 215-216(2000)171-183.

[20] A.M. Bhavikatti et al., magnetic and transport properties of cobalt ferrite, international journal of electronic engineering research, ISSN 095-6450 vol2 (2005)125-135.

[21] Shun Hua Xiao et al., low temperature auto combustion synthesis and magnetic properties of cobalt ferrite nanopowder, materials chemistry and physics 106(2007)82-87.

[22] L. Stichauer et al., optical and magneto-optical properties of copper and cobalt manganese ferrite thin film, journal of physics IV (1997) c1-729.

[23] S.S. Haryapetyan et al., microporous materials 72(2004)105.

[24] S. Arul Antory et al., journal of nuclear material295(2001)189.

[25] PEAK FIT-Version4.02, Jandel Scientific Software,1991

[26] POWD-An interactive powder diffraction data interpretation and indexing program version2.2 by E. Wu, School of Physics, Flinder University of South Australia Bedford, S.S 5042 Australia.